Applied Catalysis B: Environmental 181 (2016) 818–824

Contents lists available at ScienceDirect

Applied Catalysis B: Environmental

journal homepage: www.elsevier.com/locate/apcatb

# Photocatalytic hydrogen production from aqueous glycerol solution using $NiO/TiO_2$ catalysts: Effects of preparation and reaction conditions

Shin-ichiro Fujita, Hiroki Kawamori, Daisuke Honda, Hiroshi Yoshida, Masahiko Arai*

*Division of Applied Chemistry, Faculty of Engineering, Hokkaido University, Sapporo 060-8628, Japan*

ARTICLE INFO

*Article history:*
Received 17 June 2015
Received in revised form 27 August 2015
Accepted 30 August 2015
Available online 2 September 2015

*Keywords:*
Hydrogen
Glycerol
Water
Nickel doping
Titanium dioxide
Photocatalysis

ABSTRACT

The photocatalytic $H_2$ production from a mixture of glycerol and water over $NiO/TiO_2$ catalysts was investigated. Effects of preparation and reaction conditions were examined, including $TiO_2$ materials, NiO loading, glycerol concentration, and pH value. The rate of $H_2$ production was observed to be maximized at a certain NiO loading and at a pH value close to the zero-point charge of $TiO_2$. The influence of NiO loading may be explained by a decrease in the band gap energy and a decrease in the exposed area of $TiO_2$, which were of importance in the ranges of small and larger NiO loading, respectively. At such a pH value, the amount of surface hydroxyl groups was likely to be maximized, which could promote the adsorption of glycerol molecules via hydrogen bonding. The change of the $H_2$ production rate with the glycerol concentration was explained assuming a Langmuir adsorption model. Both water and glycerol are involved in the photocatalytic $H_2$ production with $NiO/TiO_2$ catalysts. The reaction results with $D_2O$ instead of $H_2O$ indicate that glycerol may be a main $H_2$ source. In addition, it has been found that NiO is a good choice in preparing active $TiO_2$ based catalysts as compared with the other transition metal oxides of CoO and CuO.



## 1. Introduction

Hydrogen is a clean energy carrier, and it can be produced via different processes using fossil fuels and biomass-derived materials as hydrogen sources [1–4]. The use of biomass-derived materials in the $H_2$ production is interesting and significant for effective materials recycling. Glycerol is one of biomass-derived materials, and it is produced in a large quantity as a byproduct in the transesterification reaction of vegetable oils into biodiesel fuels [5]. The photocatalytic $H_2$ production from glycerol and water is less energy-consuming reaction because it can be processed under mild conditions, as compared for example with its steam reforming at high temperatures. It is reported that $TiO_2$ based materials doped with several metal species are active catalysts for the photocatalytic $H_2$ production from glycerol, including such dopants as Pt [6–9], Au [10,11], Pd [12], and $CuO_x$ [13–17]. Montini et al. prepared Cu nanoparticles embedded in $TiO_2$ by a water-in-oil microemulsion method, and these $Cu/TiO_2$ materials were active catalysts for the $H_2$ production from glycerol and water under visible light irradiation conditions [13]. Li et al. studied the photocatalytic activity of $Cu_2O/TiO_2$ for the $H_2$ evolution in the presence of different scavengers [16]. Recently, $NiO_x$-doped $TiO_2$ materials were reported to catalyze the photocatalytic degradation of undesired organic pollutants in water [18–20]. The doping of $NiO_x$ onto the surface of $TiO_2$ is effective for the preparation of p-type ($NiO_x$) – n-type ($TiO_2$) junction [21] and these $NiO_x$-loaded $TiO_2$ materials would be useable in photocatalytic reactions.

The present authors recently showed that a NiO-supported $TiO_2$ catalyst was active for the photocatalytic production of $H_2$ from aqueous glycerol solution [22]. The $NiO/TiO_2$ samples were prepared by a conventional impregnation method in which different calcination temperatures of 250–650 °C were used to change the contact between the support ($TiO_2$) and the dispersed phase (NiO). The calcination at 450 °C was shown to produce the most active $NiO_x/TiO_2$ catalyst. The photocatalytic $H_2$ production with $NiO_x/TiO_2$ should of course depend on other catalyst preparation and reaction conditions including parent $TiO_2$ materials, NiO loading, glycerol concentration, and pH value. The effects of these factors and variables on the photocatalytic $H_2$ production have been examined, optimized, and discussed in the present follow-up work. The roles of glycerol and water molecules have also been examined and the performance of $NiO/TiO_2$ catalyst has been compared

* Corresponding author.
*E-mail address:* marai@eng.hokudai.ac.jp (M. Arai).

http://dx.doi.org/10.1016/j.apcatb.2015.08.048
0926-3373/

**Table 1**
Properties of parent $TiO_2$ and 2 wt.% NiO-loaded $TiO_2$ samples prepared and their photocatalytic performance for $H_2$ production from glycerol solution.[a]

| Entry | Sample[b] | *A*:*R*[c] | $TiO_2$ crystallite size[d] (nm) | Surface area ($m^2\ g^{-1}$) | $H_2$ evolution ($\mu mol\ g^{-1}\ h^{-1}$) | ($\mu mol\ m^{-2}\ h^{-1}$) |
|---|---|---|---|---|---|---|
| 1 | $TiO_2$(1) | 7:3 | 19 | 53 | | |
| 2 | NiO/$TiO_2$(1) | 7:3 | 20 | 54 | 1230 | 22.8 |
| 3 | $TiO_2$(2) | 10:0 | 51 | 11 | | |
| 4 | NiO/$TiO_2$(2) | 10:0 | 51 | 13 | 258 | 19.8 |
| 5 | $TiO_2$(3) | 10:0 | 9 | 125 | | |
| 6 | NiO/$TiO_2$(3) | 10:0 | 11 | 90 | 459 | 5.1 |
| 7 | $TiO_2$(4) | 0:10 | 16 | 90 | | |
| 8 | NiO/$TiO_2$(4) | 0:10 | –[e] | 59 | –[f] | –[f] |

[a] Reaction conditions: water 10 $cm^3$, glycerol 2 $cm^3$ (glycerol concentration 2.28 mol $dm^{-3}$), catalyst 20 mg, temperature 50 °C, time 8 h.
[b] $TiO_2$(1): Catalysis Society of Japan (CSJ) JRC-4, $TiO_2$(2): Sigma–Aldrich, $TiO_2$(3): Home-made by a solvothermal method [23–25], $TiO_2$(4): CSJ JRC-6.
[c] anatase/rutile ratio [26–28].
[d] Determined by XRD.
[e] Not determined.
[f] Inactive.

with that of other transition metal (Co, Cu) oxide doped $TiO_2$ ones prepared in similar manners.

## 2. Experimental

The experimental procedures of catalyst preparation, characterization, and activity measurement used are described in detail in a previous work [22]. In brief, four different $TiO_2$ materials were used, which were $TiO_2$(1) obtained from Catalysis Society of Japan (CSJ) (JRC-4), $TiO_2$(2) purchased from Sigma–Aldrich, $TiO_2$(3) prepared by a solvothermal method in the laboratory [23–25], and $TiO_2$(4) from CSJ (JRC-6). Their structural and textural properties will be given later (Table 1). Nickel species was loaded onto these $TiO_2$ materials by a conventional impregnation using $Ni(NO_3)_2{\cdot}6H_2O$ (Wako) as a precursor followed by calcination in air at an optimized temperature of 450 °C. For comparison, CoO and CuO loaded $TiO_2$ samples were also prepared using $Co(CH_3COO)_2{\cdot}4H_2O$ (Wako) and $Cu(NO_3)_2{\cdot}3H_2O$ (Wako) as precursors, respectively. The $NiO_x/TiO_2$ samples prepared, which were different in the parent $TiO_2$ and NiO loading, were characterized by X-ray diffraction (Rigaku RINT2200), field-emission transmission electron microscopy (FE-TEM, JEOL JEM-2010F), $N_2$ adsorption (Quantachrome NOVA 1000), and UV–vis spectroscopy (Shimadzu UV-3100). The photocatalytic activity of those NiO/$TiO_2$ catalysts prepared was measured for the $H_2$ production from a mixture of glycerol and water in a laboratory-made high-pressure batch reactor of 50 $cm^3$. The reactor was loaded with NiO/$TiO_2$ sample, glycerol (Wako), and distilled water (Wako), purged by passing $N_2$ (0.5 MPa) three times, and closed and then the reactor was heated by a heating tape while stirring the reaction mixture with a magnetic stirrer. When the temperature reached to a reaction temperature of 50 °C, the reaction mixture was illuminated using a 500 W high-pressure Hg lamp (Ushio USH-500SC). The gaseous products evolved after the photocatalytic reaction were collected in a gas trap and analyzed with gas chromatograph (Shimadzu GC-8A) and mass spectrometry (MicrotracBEL BELCAT-A, BELMass).

## 3. Results and discussion

The NiO/$TiO_2$ samples prepared were used to examine the influence of parent $TiO_2$ materials, NiO loading, glycerol concentration, and initial pH on the photocatalytic $H_2$ evolution from a mixture of glycerol and water (Scheme 1). In addition, the roles of glycerol and water have been discussed, and the performance of NiO/$TiO_2$ samples has been compared with that of CoO/$TiO_2$ and CuO/$TiO_2$ ones prepared in similar procedures.

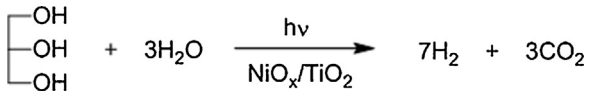


**Scheme 1.** Photocatalytic $H_2$ production from glycerol and water.

### 3.1. Screening of $TiO_2$ materials

Four different $TiO_2$ materials loaded with NiO in 2.0 wt.% were prepared and tested for the photocatalytic $H_2$ production from an aqueous glycerol solution. These samples were prepared via calcination at a temperature of 450 °C, at which the photocatalytic performance was maximal as reported previously [22]. Table 1 shows structural and textural properties of parent and NiO-loaded $TiO_2$ samples, and Fig. 1 gives their XRD patterns. Table 1 also present the results of photocatalytic $H_2$ evolution for the NiO-loaded $TiO_2$ samples. The parent $TiO_2$ samples were observed to be even less active under the conditions used. The rate of $H_2$ production was in the order of NiO/$TiO_2$(1) > NiO/$TiO_2$(3) > NiO/$TiO_2$(2) » NiO/$TiO_2$(4) on the unit weight basis and NiO/$TiO_2$(1) ≈ NiO/$TiO_2$(2) > NiO/$TiO_2$(3) » NiO/$TiO_2$(4) on the unit surface area basis. The former three samples of NiO on anatase and anatase-rich $TiO_2$ materials were active for the $H_2$ production (entries 2, 4, 6) but the latter one of NiO on rutile $TiO_2$(4) was inactive (entry 8). In addition to $H_2$, a few carbon-containing species, such as CO, $CO_2$, and $CH_4$, were observed to form and the total amount of these species did not depend so much on the catalysts used. For the most active catalyst, NiO/$TiO_2$(1) (entry 2), the evolution of CO, $CO_2$, and $CH_4$ was 106, 41, and 19 mmol $g^{-1}\ h^{-1}$, respectively. In the case of less active NiO/$TiO_2$(2) (entry 4), the total amount of the carbon-containing species (CO » $CO_2$ > $CH_4$) was comparable to that of $H_2$. From those results, $TiO_2$(1) was then selected and used to further examine the influence of preparation and reaction conditions in the present work ($TiO_2$(1) will be simply denoted as $TiO_2$ hereinafter).

### 3.2. Influence of NiO loading

Fig. 2 shows the rate of photocatalytic $H_2$ production against the NiO loading. The $H_2$ evolution rate was about 500 $\mu mol\ g^{-1}\ h^{-1}$ for $TiO_2$ alone under the conditions used, and it was enhanced by the NiO loading, which was maximized at around 2 wt.% NiO. The loading of NiO was not found to change the structure of $TiO_2$ (Fig. 3) and its surface area. For 2 wt.% NiO loaded $TiO_2$, no appreciable NiO diffraction was detected, indicating that NiO was highly dispersed on the surface of $TiO_2$. When the amount of NiO loaded was further increased, NiO diffraction was detected and NiO existed in the form of small crystallites. The high dispersion of NiO was also confirmed

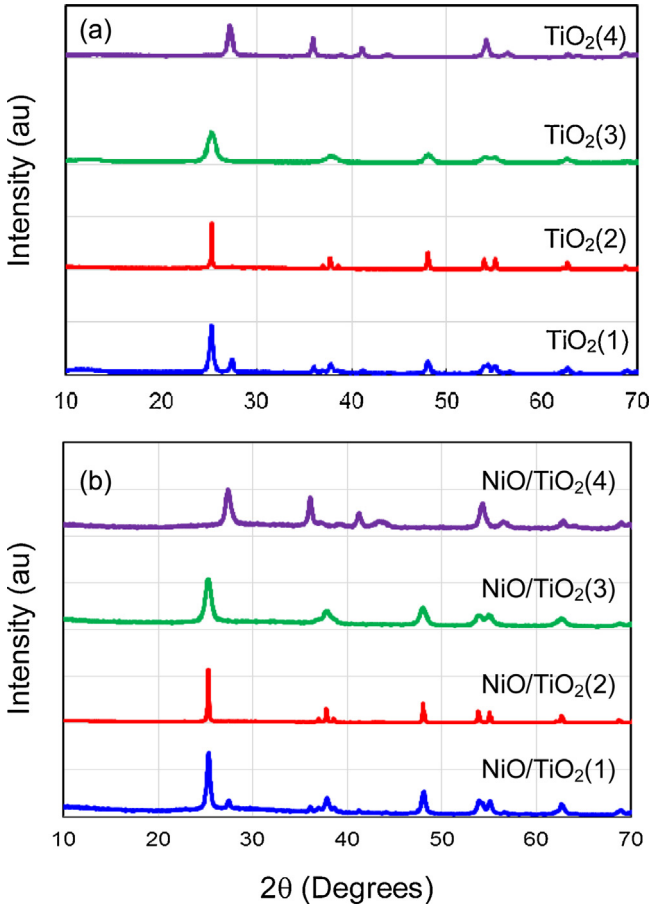


**Fig. 1.** XRD patterns of parent $TiO_2$ samples (a) and 2.0 wt.% NiO-loaded $TiO_2$ samples (b).

by FE-TEM for 2 wt.% and 10 wt.% $NiO/TiO_2$ samples. It was observed that small NiO particles with diameter in a few nanometers were dispersed on the surface of $TiO_2$ (TEM pictures are presented in Supporting information).

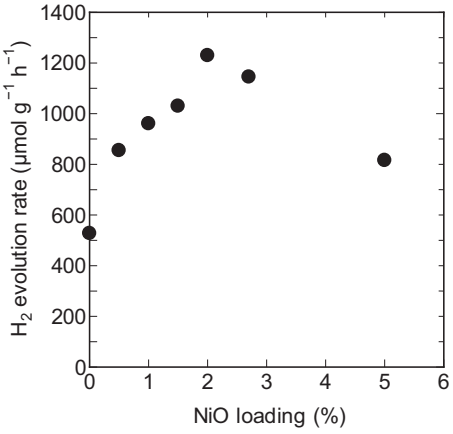


**Fig. 2.** Influence of NiO loading on the rate of $H_2$ evolution for $NiO_x/TiO_2$ catalysts. Reaction conditions: water 10 $cm^3$; glycerol 2 $cm^3$ (glycerol concentration 2.28 mol $dm^{-3}$); catalyst 20 mg; temperature 50 °C; time 8 h.

UV–vis measurements were made to characterize those $NiO/TiO_2$ samples. Fig. 4 gives UV–vis spectra collected, which were different depending on the NiO loading. These UV–vis results were used to estimate the band gap energy, $E_g$, which was observed to merely decrease with an increase in the NiO loading (Fig. 5). In Fig. 6, the $H_2$ evolution rate is plotted against the $E_g$ value for $NiO/TiO_2$ samples in which the NiO loading is 2 wt.% or smaller and the calcination temperature is 450 °C or 250 °C. A good correlation exists between the $H_2$ evolution rate and the $E_g$ value. The results of Fig. 2 may be explained by the change in the $E_g$ value for the $NiO/TiO_2$ samples in which the NiO loading is ≤2.0 wt.%. When the NiO loading is increased, the $E_g$ value further decreases (Fig. 5), but the photocatalytic $H_2$ evolution rate does not increase (Fig. 2). This may be due to a decrease in the exposed area of $TiO_2$ that can be illuminated by the light with an increase in the NiO loading. Recently, Li et al. reported the same conclusion on the influence of NiO loading in the photocatalytic water splitting over $NiO/TiO_2$ composite nanofibers using methanol as sacrificial agent [29]. Li et al. used $Cu_2O/TiO_2$ catalysts for the photocatalytic water splitting using different scavengers [16]. They measured $E_g$ values for

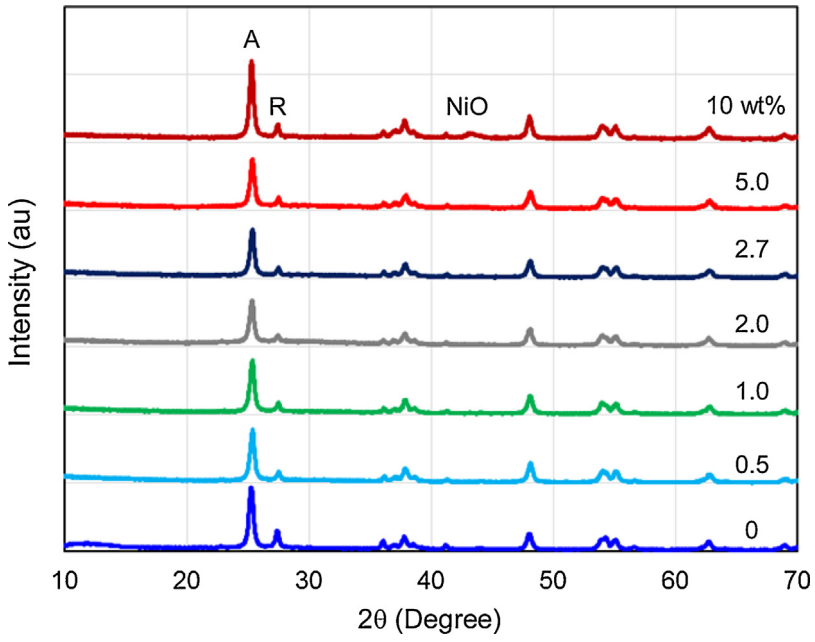


**Fig. 3.** XRD patterns of $NiO_x/TiO_2$ samples different in the NiO loading.

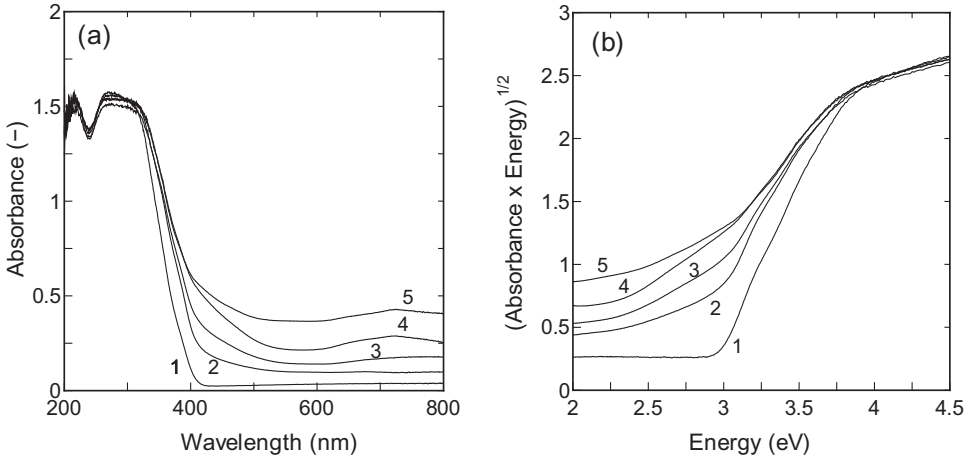


**Fig. 4.** (a) Typical UV–vis spectra of $NiO/TiO_2$ samples different in NiO loading. (b) Plot of (absorbance × energy)$^{1/2}$ against energy obtained from the data (a). NiO loading (wt.%): 0 (line 1), 1.0 (2), 2.5 (3), 5.0 (4), and 10.0 (5).

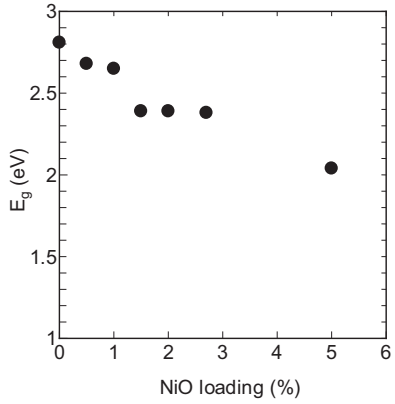


**Fig. 5.** Influence of NiO loading on the band gap energy, $E_g$, of $NiO/TiO_2$ samples.

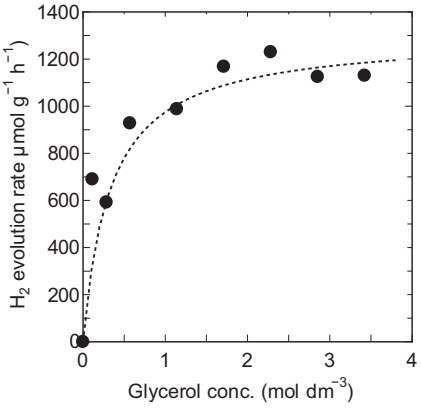


**Fig. 7.** Plot of the rate of $H_2$ evolution against the initial concentration of glycerol. Reaction conditions: 2.0 wt.% NiO-loaded $TiO_2$, 20 mg; water + glycerol 12 cm$^3$; temperature 50 °C; time 8 h.

the catalysts different in the $Cu_2O$ loading and observed that the $E_g$ value decreased with an increase in the amount of $Cu_2O$ loaded, in accordance with the trend of Fig. 5.

The relationship between the $H_2$ evolution rate and the $E_g$ value was further examined by using other $NiO/TiO_2$ samples different in NiO loading and calcination temperature, which should change the state of $TiO_2$–NiO contact, and thus, change the $E_g$ value. The results

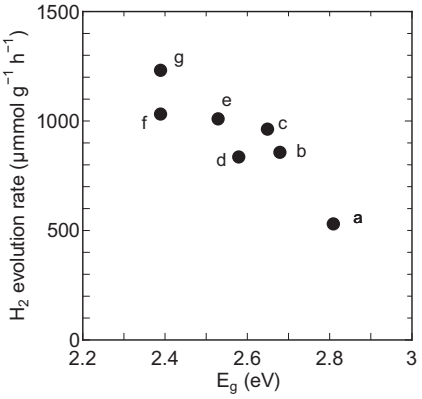


**Fig. 6.** Plot of the rate of $H_2$ evolution against the band gap energy $E_g$ for several $NiO_x/TiO_2$ samples different in NiO loading and calcination temperature. NiO loading (wt%) and calcination temperature (°C): 0, 450 (a); 0.5, 450 (b); 1.0, 450 (c); 2.0, uncalcined (d); 2.0, 250 (e); 1.5, 450 (f); 2.0, 450 (g).

(Fig. 6) show that the rate of $H_2$ evolution tends to increase with a decrease in the $E_g$ value. Hence, the $E_g$ is a significant factor determining the activity of $NiO/TiO_2$ for the photocatalytic $H_2$ production from aqueous glycerol solution under the present reaction conditions. It is assumed that the loading of NiO (p-type semiconductor) to $TiO_2$ (n-type conductor) produces a p–n junction through which an internal electric field appears at the interfacial layer between the NiO and $TiO_2$ phases [30]. This should reduce the energy of optical excitation ($E_g$) and retard the undesired recombination of electrons and holes produced by the optical excitation of the $NiO/TiO_2$ catalyst.

### 3.3. Influence of glycerol concentration, pH, and $D_2O$

Then, the influence of reaction conditions on the $H_2$ production was examined. Fig. 7 shows the influence of initial glycerol concentration on the photocatalytic $H_2$ evolution with the most active 2.0 wt.% $NiO/TiO_2$ catalyst. The rate of $H_2$ evolution increases almost linearly with the glycerol concentration when it is small (<0.5 mol dm$^{-3}$). When it is further increased, the $H_2$ evolution rate also increases but not so largely and then levels off at around 1200 μmol g$^{-1}$ h$^{-1}$ under the conditions used. The change of the $H_2$ evolution rate with the glycerol concentration observed may indicate that the adsorption of glycerol on the catalyst obeys the Langmuir-type adsorption and the amount of glycerol adsorbed

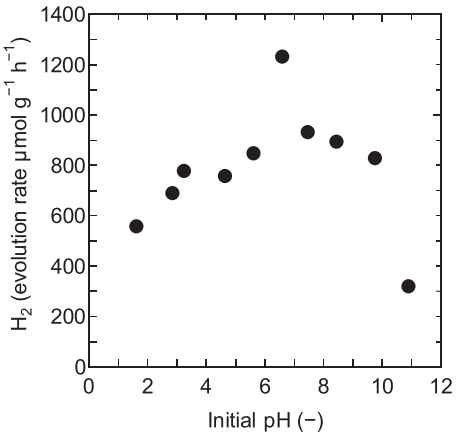


**Fig. 8.** Influence of initial pH value on the rate of $H_2$ evolution for 2.0 wt.% NiO-loaded $TiO_2$ catalyst: Reaction conditions: catalyst 20 mg; water 10 $cm^3$; glycerol 2 $cm^3$ (glycerol concentration 2.28 mol $dm^{-3}$); temperature 50 °C; time 8 h. The pH value of aqueous glycerol solution was changed with hydrochloric and sodium hydroxide solutions.

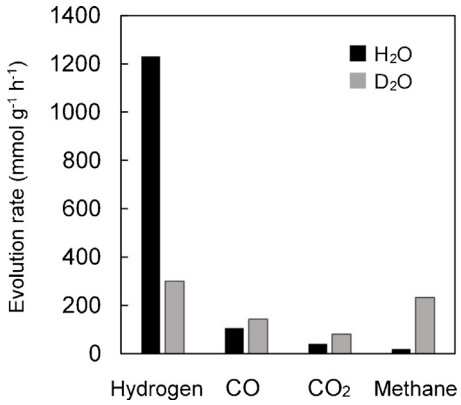


**Fig. 9.** The rate of evolution of gaseous products in the photocatalytic reaction of glycerol with either $H_2O$ or $D_2O$. Reaction conditions: 2.0 wt.% NiO/$TiO_2$ catalyst 20 mg; water 10 $cm^3$; glycerol 2 $cm^3$ (glycerol concentration 2.28 mol $dm^{-3}$); temperature 50 °C; time 8 h.

determines the rate of photocatalytic $H_2$ production. Fig. 7 gives a dotted line calculated through the rate of $H_2$ evolution = $k_1K_aC_0/(1+K_aC_0)$, in which $C_0$ is glycerol concentration, $k_1$ is pseudo first order rate constant (1.3 mol $g^{-1}$ $h^{-1}$), and $K_a$ is equilibrium constant for glycerol adsorption/desorption (3.0 $dm^3$ $mol^{-1}$). The observed experimental results of Fig. 7 can be correlated by the Langmuir adsorption model. Lalitha et al. studied the photocatalytic production of $H_2$ from aqueous glycerol solution over $Cu_2O/TiO_2$ [15]. They observed that with increasing glycerol concentration, the rate of $H_2$ evolution increased, similar to the result of Fig. 7, had a maximum, and then slightly decreased. It is noted that this behavior resulted from the saturation of active sites by glycerol [31].

Next, the influence of initial pH value was examined with the same catalyst. Fig. 8 shows that the rate of $H_2$ evolution is maximal at a pH value of about 6.6, which is close to the pH at the zero-point charge of $TiO_2$ [32,33], under the reaction conditions used. It is assumed that the quantity of surface hydroxyl groups, which can promote the adsorption of glycerol molecules through hydrogen bonding, is maximized at such a pH value, causing a maximum in the rate of $H_2$ evolution. Those results (Figs. 7 and 8) indicate the significance of the adsorption of glycerol on the surface of NiO/$TiO_2$ catalyst in determining the rate of photocatalytic $H_2$ evolution. In contrast to the large change of the $H_2$ evolution, the total amount of the carbon-containing species of CO, $CO_2$, and $CH_4$ evolved was not observed to change so much with the glycerol concentration and the pH condition.

To examine the role of water, $D_2O$ was used instead of $H_2O$ for the photocatalytic $H_2$ evolution with the most active NiO/$TiO_2$ catalyst. The results obtained with $D_2O$ and $H_2O$ are compared in Fig. 9. When $D_2O$ was used, the rate of hydrogen evolution was significantly deceased, which was about one-fourth of the rate with $H_2O$, and the amounts of methane, CO, and $CO_2$ evolved were increased. In particular, the amount of $CH_4$ evolved was comparable to that of hydrogen evolved in the reaction in $D_2O$. The gaseous hydrogen species after a photocatalytic reaction with $D_2O$ under the same conditions given for Fig. 9 except for a longer reaction time of 10 h were analyzed by mass spectrometry. $H_2$, HD, and $D_2$ were detected to form but the relative amount of either HD or $D_2$ was about 1.5% as compared to that of $H_2$. Therefore, glycerol should be a main source for hydrogen, and water also could affect the hydrogen production as suggested by Fig. 9.

### 3.4. Hydrogen production from aqueous glycerol solution with NiO/$TiO_2$

As discussed above, the loading of NiO to $TiO_2$ decreases the $E_g$ value, probably due to the formation of internal electric field at the interfacial layer between the NiO and $TiO_2$ phases. In other words, the optical excitation can occur with a smaller energy by the presence of NiO. When the NiO/$TiO_2$ catalyst is illuminated by light, pairs of electron and hole are produced and electrons formed would move to the NiO phase, which could retard the undesired recombination of electrons and holes [17]. Thus, the photocatalytic activity of $TiO_2$ should be enhanced by the loading of NiO on its surface. Figs. 7 and 8 indicate the importance of the adsorption of glycerol; UV–vis measurements were made for a selected NiO/$TiO_2$ sample before and after the adsorption of glycerol, which was confirmed by FTIR, but the $E_g$ value did not change by the presence of glycerol (the UV–vis and FTIR results are presented in Supporting information).

Furthermore, the above-mentioned results with $D_2O$ indicate that glycerol may be a main hydrogen source. Although there is no experimental evidence for that hydrogen is also produced from glycerol in glycerol + $H_2O$ mixture, Figs. 7 and 8 show the significance of glycerol adsorption on the NiO/$TiO_2$ catalyst, from which glycerol is assumed to be the hydrogen source. The authors attempted to analyze the liquid phase after the reaction for a longer time of 100 h by GC and GC–MS but they failed to detect any organic compounds other than the substrate, glycerol. The gaseous carbon-containing species of CO, $CO_2$, and $CH_4$ were detected to form but in small quantities. The amounts of CO, $CO_2$, and $CH_4$ formed with the most active NiO/$TiO_2$ catalyst under the conditions given in Table 1 were 106, 41, and 19 mmol $g^{-1}$ $h^{-1}$; the total amount of these C-containing species was <1/10 of the amount of $H_2$ formed. For pure water in the absence of glycerol, these species were not detected. Therefore, these C-containing species should originate from glycerol.

The results of Fig. 9 with $H_2O$ and $D_2O$ indicate some effect of water molecules on the photocatalytic production of hydrogen in aqueous glycerol solution. However, no clear explanation can be found at present. In the literature, there are several works on photocatalytic water splitting using alcohols as sacrificial agents. Methanol and ethanol are known to act as sacrificial agents promoting the photocatalytic water splitting, in which these are oxidized by consumption of holes [16,34]. Li et al. studied the photocatalytic water splitting with $Cu_2O/TiO_2$ in the presence of different scavengers [16]. The effectiveness for the $H_2$ production was in the order of methanol > glycol ≈ glycerol > anhydrous ethanol but not so sig-

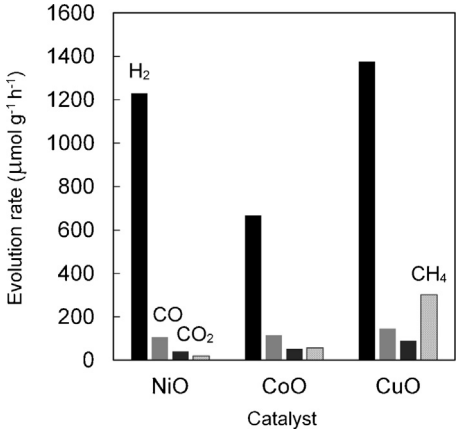


**Fig. 10.** Comparison among $TiO_2$-supported NiO, CoO, and CuO catalysts in the performance for the $H_2$ production from aqueous glycerol solution. Metal oxide loading 2.0 wt.%. Reaction conditions: catalyst 20 mg; water 10 $cm^3$; glycerol 2 $cm^3$ (glycerol concentration 2.28 mol $dm^{-3}$); temperature 50 °C; time 8 h.

nificant. They note that the scavengers react only with the hydroxyl radical but not with its precursor hole because water is easier to be adsorbed on the catalyst of $Cu_2O/TiO_2$ compared to the scavenger molecules [16]. It is speculated in our case that the adsorption of water molecules on the $NiO/TiO_2$ catalyst influences the adsorption of glycerol molecules and/or water molecules are involved in the photocatalytic production of hydrogen from glycerol. These indirect and/or direct effects of water might be responsible for the isotope effects observed (Fig. 9).

Lalitha et al. propose reaction mechanisms for the photocatalytic $H_2$ production from aqueous glycerol solution over $Cu_2O/TiO_2$ catalyst [15]; glycerol is attacked by hydroxyl radical formed from water and hole and, through several hydration and dehydration steps forming smaller intermediates, changes to $H_2$ and $CO_2$. According to these mechanisms, $H_2$ would result from glycerol and water. Petala et al. observed the formation of such intermediates as acetone, acetaldehyde, and formic acid in addition to $H_2$ and $CO_2$ in the photocatalytic reforming of glycerol with $Cu_xO/TiO_2$ catalysts [17]. In our case using $NiO/TiO_2$ catalysts, the stoichiometric reaction of Scheme 1 does not occur and the results with $D_2O$ suggest that hydrogen mainly comes from glycerol rather than water. To elucidate reaction mechanisms, further works are needed, for example, those using labelled glycerol.

### 3.5. Comparison with other metal-loaded $TiO_2$ catalysts

Finally, the performance of NiO loaded $TiO_2$ catalyst was compared with that of other transition metal (Co, Cu) loaded $TiO_2$ ones, which were prepared in similar preparation procedures using $TiO_2$(1) (Table 1) and $Co(CH_3COO)_2{\cdot}4H_2O$ and $Cu(NO_3)_2{\cdot}3H_2O$ as precursors, respectively. For these samples, the metal loading was 2.0 wt.%, and the calcination temperature was 450 °C, which were optimized for $NiO/TiO_2$ catalyst in the previous work [22]. The results obtained with the three metal loaded $TiO_2$ catalysts so prepared are compared in Fig. 10. When compared with $NiO/TiO_2$, the rate of $H_2$ evolution with $CuO/TiO_2$ was comparable but that with $CoO/TiO_2$ was even smaller. The formation of such carbon containing products as CO, $CO_2$, and $CH_4$ were observed for the three catalysts and a larger amount of $CH_4$ was formed with $CuO/TiO_2$ as compared to $NiO/TiO_2$ and $CoO/TiO_2$. For the CuO-loaded $TiO_2$ catalyst, undesired reactions might have occurred under the conditions used. Gui et al. studied the photocatalytic steam reforming of $CO_2$ over CuO, NiO, and CoO loaded $TiO_2$ catalysts [35]. They found that the rate of $CH_4$ formation with $CuO/TiO_2$ was larger compared to the other catalysts; that is, it has a larger activity for the methanation of $CO_2$. Thus, NiO is a good choice for preparing active $TiO_2$ based materials for the photocatalytic $H_2$ production from aqueous glycerol solution.

## 4. Conclusions

The loading of NiO onto the surface of $TiO_2$ reduces the band gap energy ($E_g$) of $NiO/TiO_2$ catalyst, and the $E_g$ value decreases with increasing NiO loading. This enhances the photocatalytic activity of $NiO/TiO_2$ for the $H_2$ production from a mixture of water and glycerol. At a larger NiO loading, however, the rate of $H_2$ production becomes lowered probably due to a decrease in the exposed surface area of $TiO_2$ that can be illuminated by light. With increasing glycerol concentration the $H_2$ evolution increases linearly, slightly, and then levels off, which can be correlated by Langmuir-adsorption model. The rate of $H_2$ evolution depend on the pH of the mixture and is maximized at a certain pH close to the zero-point charge. These results indicate the significance of the adsorption of glycerol in the photocatalytic $H_2$ production over $NiO/TiO_2$. The results with $D_2O$ shows an isotope effect on the evolution of hydrogen, and $H_2$ was main hydrogen species produced with a smaller amount (1.5%) of either HD or $D_2$. It is likely that glycerol is a main hydrogen source and water also could affect the hydrogen production. NiO is a good choice in preparing active $TiO_2$ based catalysts as compared with the other transition metal oxides of CoO and CuO loaded to $TiO_2$ in the same manners.

## Acknowledgement

The authors are thankful to Mr. Y. Onodera and Prof. K. Shimizu of Hokkaido University for UV–vis and FTIR measurements and mass spectrometry measurements, respectively.

## Appendix A. Supplementary data

Supplementary data associated with this article can be found, in the online version, at http://dx.doi.org/10.1016/j.apcatb.2015.08.048.

## References

[1] L. Gradisher, B. Dutcher, M. Fan, Appl. Energy 139 (2015) 335–349.
[2] M. Cargnello, A. Gasparotto, V. Gombac, T. Montini, D. Barreca, P. Fornasiero, Eur. J. Inorg. Chem. (2011) 4309–4323.
[3] K. Shimura, H. Yoshida, Energy Environ. Sci. 4 (2011) 2467–2481.
[4] R.M. Navarro, M.C. Sánchez-Sáncez, M.C. Alvarez-Galvan, F. del Valle, J.L.G. Fierro, Energy Environ. Sci. 2 (2009) 35–54.
[5] C.H.C. Zhou, J.N. Beltramini, Y.X. Fan, G.Q.M. Lu, Chem. Soc. Rev. 37 (2008) 527–549.
[6] V.M. Daskalaki, D.I. Kondarides, Catal. Today 144 (2009) 75–80.
[7] D.I. Kondarides, V.M. Daskalki, A. Patsoura, X.E. Verykios, Catal. Lett. 122 (2008) 26–32.
[8] N. Fu, G. Lu, Catal. Lett. 127 (2009) 319–322.
[9] N. Luo, Z. Jiang, H. Shi, F. Cao, T. Xiao, P.P. Edwards, Int. J. Hydrog. Energy 34 (2009) 125–129.
[10] E. Toboada, I. Angurell, J. Llorca, J. Photochem. Photobiol. A Chem. 281 (2014) 35–39.
[11] F. Gärtner, S. Losse, A. Boddien, M.-M. Pohl, S. Denurra, H. Junge, M. Beller, ChemSusChem 5 (2012) 530–533.
[12] M. Bowker, P.R. Davies, L.S. Al-Mazroai, Catal. Lett. 128 (2009) 253–255.
[13] T. Montini, V. Gombac, L. Sordelli, J.J. Delgado, X. Chen, G. Adami, P. Fornasiero, ChemCatChem 3 (2011) 574–577.
[14] V. Gombac, L. Sordelli, T. Montini, J.J. Delgado, A. Adamski, G. Adami, M. Cargnello, S. Bernal, P. Fornasiero, J. Phys. Chem. A 114 (2010) 3916–3925.
[15] K. Lalitha, G. Sadanandam, V.D. Kumari, M. Subrahmanyam, B. Sreedhar, N.Y. Hebalkar, J. Phys. Chem. C 114 (2010) 22181–22189.
[16] Y. Li, B. Wang, S. Liu, X. Duan, Z. Hu, Appl. Surf. Sci. 324 (2015) 736–744.
[17] A. Petala, E. Ioannidou, A. Georgaka, K. Bourikas, D.I. Kondarides, Appl. Catal. B Environ. 178 (2015) 201–209.
[18] L. Ren, Y. Zeng, D. Jiang, Solid State Sci. 12 (2010) 138–143.
[19] C. Chen, C. Liao, K. Hsu, Y. Wu, J.C. Wu, Catal. Commun. 12 (2011) 1307–1310.
[20] A. Iwaszuki, M. Nolan, Q. Jin, M. Fujishima, H. Tada, J. Phys. Chem. C 117 (2013) 2709–2718.

[21] A. Kudo, K. Domen, K. Maruya, T. Onishi, Chem. Phys. Lett. 133 (1987) 517–519.
[22] R. Liu, H. Yoshida, S. Fujita, M. Arai, Appl. Catal. B Environ. 144 (2014) 41–45.
[23] P. Kittisakmontree, H. Yoshida, S. Fujita, M. Arai, J. Panpranot, Catal. Commun. 58 (2015) 70–75.
[24] N. Comsup, J. Panpranot, P. Praserthdam, Catal. Commun. 11 (2010) 1238–1243.
[25] N. Comsup, J. Panpranot, P. Praserthdam, J. Ind. Eng. Chem. 16 (2010) 703–707.
[26] G. Colón, J.M. Sánchez-España, M.C. Hidalgo, J.A. Navío, J. Photochem. Photobio. A Chem. 179 (2006) 20–27.
[27] T.L. Thompson, J.T. Yates Jr., Chem. Rev. 106 (2006) 4428–4453.
[28] H.P. Klug, L.E. Alexander, X-ray Diffraction Procedures for Polycrystalline and Amorphous Materials, John Wiley, London, UK, 1954, p. 491.
[29] L. Li, B. Cheng, Y. Wang, J. Yu, J. Colloid Interface Sci. 449 (2015) 115–121.
[30] C. Chen, C. Liao, K. Hsu, Y. Wu, J.C.S. Wu, Catal. Commun. 12 (2011) 1307–1310.
[31] N. Strataki, V. Bekiari, D.L. Kondarides, P. Liano, Appl. Catal. B Environ. 77 (2007) 184–189.
[32] K. Selvam, M. Muruganandham, I. Muthuvel, M. Swaminathan, Chem. Eng. J. 128 (2007) 51–57.
[33] L. Zang, P. Qu, J. Zhao, T. Shen, H. Hidaka, J. Mol. Catal. A Chem. 120 (1997) 235–245.
[34] H. Ahmad, S.K. Kamarudin, L.J. Minggu, M. Kassim, Renew. Sustain. Energy Rev. 43 (2015) 599–610.
[35] M.M. Gui, S.-P. Chai, A.R. Mohamed, Appl. Surf. Sci. 319 (2014) 37–43.